Molecular Orbital Study of the Interaction between MgATP and the Myosin Motor Domain: The Highest Occupied Molecular Orbitals Indicate the Reaction Site of ATP Hydrolysis

Hiroshi Kagawa*,† and Kazuhide Mori‡

Physics Laboratory, Nippon Medical School, 2-297-2 Kosugi, Kawasaki 211-0063, Japan, and Waseda Computational Science Consortium, c/o Prof. K. Suzuki, Takachiho University, Suginami, Tokyo 168-8508, Japan

Received: April 1, 1999; In Final Form: June 29, 1999

We constructed a model structure of Mg−adenosine triphosphate (MgATP) and the surrounding portion of myosin by using the X-ray crystal structure of the myosin motor domain bound to the stable MgATP analogue, MgADP−BeF_x, and by adding hydrogen atoms and replacing beryllium with phosphorus and fluorine with oxygen. The positions of the hydrogen atoms were determined by optimization using the semiempirical molecular orbital program MOPAC 97. Analysis of the electronic states of the model structure revealed that the highest occupied molecular orbitals (HOMO) indicate that the reaction site of the ATP hydrolysis is the nonbridging γ-phosphoryl oxygen atoms and confirmed that H_2O(1181) is the hydrolytic water. Thus, hypothetical mechanisms of the initial phase of the hydrolysis are proposed.

1. Introduction

The muscle protein myosin moves using energy from the hydrolysis of adenosine triphosphate (ATP). Myosin binds ATP and hydrolyzes it to produce adenosine diphosphate (ADP) and phosphoric acid. These products are then released. Repeating this process, myosin filaments slide on actin filaments. Many studies have pursued investigation of the relationship between ATP hydrolysis and the structural change of myosin.[1] The time and space-resolving power of the presently available methods, however, is not enough to investigate this relationship on a detailed molecular level. At the same time, an electrotheoretical understanding of the mechanochemical coupling of how a myosin molecule binds ATP, hydrolyzes it, and replaces it with the next ATP has not yet been obtained.

Computer processing capabilities have improved remarkably in recent years so that quantum chemical calculations of even biomolecules are gradually becoming possible. Such calculations for the subject matter, however, have only been performed for an ATP- or MgATP-independent system, or parts of them.[2−7] As a primary step to understand the mechanochemical coupling, in the present paper, we performed the calculation of an expanded system, MgATP with its surrounding portions of myosin.

X-ray crystal structures of the myosin motor domain-binding MgATP were obtained using MgATP analogues as reported by Fisher et al.[8] Using a portion of one of these structures that mimics the ATP-bound state, we constructed a model structure of MgATP bound to the myosin motor domain for molecular orbital calculations. The molecular orbital calculations were performed using the MOPAC 97 program based on the semiempirical molecular orbital method.[9,10] Because the positions of hydrogen atoms cannot be experimentally determined, hydrogen atoms were added to the chemically proper sites of the structure and their positions were determined by optimization of hydrogen atoms with MOPAC 97. The model structure of the MgATP-bound myosin motor domain consists of MgATP, nine amino acid residues of myosin near the phosphate portion of MgATP, and seven water molecules near MgATP. Total energies of MgATP, its surrounding structure, and their complex, namely, the model structure, were calculated and then analyzed as to whether the complex is stable and how the electronic states are changed. Analyzing the electronic states of the model structure, we confirmed that H_2O(1181) is the hydrolytic water, found that HOMOs (highest occupied molecular orbitals) indicate that the reaction site of the ATP hydrolysis is nonbridging oxygen atoms of γ-phosphate in the model structure, and proposed hypothetical mechanisms of the initial phase of the hydrolysis.

2. Methods of Calculations

We constructed a model structure of MgATP with the myosin motor domain for semiempirical molecular orbital calculations using the three-dimensional structure of MgADP−BeF_x-S1Dc, the complex of MgATP analogue, and the truncated myosin head from *Dictyostelium discoideum* myosin II (X-ray coordinate file: 1MMD of the Protein Data Bank (PDB)).[8] The MgATP analogue, MgADP−BeF_x, is stable so that MgADP−BeF_x-S1Dc was used as an analogue of MgATP-S1Dc for X-ray crystallography. Because of the limited number of atoms available in WinMOPAC in which the MOPAC 97 program is implemented, only MgADP−BeF_x ($x = 3$ in the PDB 1MMD data), nine amino acid residues of the P-loop (phosphate binding loop),[11] and seven oxygen atoms of waters [H_2O(1001), H_2O(1002), H_2O(1033), H_2O(1175), H_2O(1181), H_2O(1343), and H_2O(1344)] near the ATP analogue were selected. Selected amino acid sequences are a sequence of the P-loop composed of six amino acid residues, Ser181-Gly182-Ala183-Gly184-Lys185-Thr186, and a sequence of three amino acid residues, Ser236-Ser237-Arg238, located near the triphosphate portion of ADP−BeF_x.

† Nippon Medical School. E-mail: kagawa@nms.ac.jp.
‡ Waseda Computational Science Consortium. E-mail: UR6K-MR@asahi-net.or.jp.

10.1021/jp991117g CCC: $18.00
Published on Web 08/03/1999

TABLE 1: Locations and Net Atomic Charges of 34 Selected Atoms in the Model Complex[a]

portion	MOPAC no.	atom	location	PDB label	PDB no.	charge (complex)	charge (separated)
MgATP-2w	23	P	ATP	Pα	5883	2.199	2.163
	24	O	ATP	O2α	5885	−1.056	−1.060
	25	O	ATP	O3α	5886	−1.001	−0.981
	27	P	ATP	Pβ	5879	2.315	2.270
	28	O	ATP	O2β	5881	−0.963	−0.927
	29	O	ATP	O3β	5882	−0.972	−0.952
	30	Mg	Mg	Mg	5878	0.660	0.590
	31	P	ATP	Be	5906	2.185	2.098
	34	O	ATP	F3	5909	−0.959	−0.876
	35	O	H_2O(1001)	O	5910	−0.392	−0.386
	36	O	H_2O(1002)	O	5911	−0.314	−0.315
	37	O	ATP	F1	5907	−1.031	−1.057
	106	O	ATP	O1α	5884	−1.000	−1.002
	109	O	ATP	O1β	5880	−0.981	−0.980
	110	O	ATP	F2	5908	−1.020	−1.009
	113	H	H_2O(1001)	(O)		0.216	0.219
	114	H	H_2O(1001)	(O)		0.300	0.307
	115	H	H_2O(1002)	(O)		0.252	0.261
	116	H	H_2O(1002)	(O)		0.239	0.227
cage	5	O	H_2O(1343)	O	6252	−0.427	−0.359
	13	O	H_2O(1033)	O	5942	−0.469	−0.359
	22	O	H_2O(1344)	O	6253	−0.421	−0.358
	26	O	H_2O(1175)	O	6084	−0.466	−0.354
	40	O	H_2O(1181)	O	6090	−0.456	−0.320
	63	O	Ser 236	Oγ	1851	−0.396	−0.302
	70	C	Lys 185	Cϵ	1491	−0.065	−0.117
	73	N	Lys 185	Nζ	1492	−0.177	−0.022
	87	O	Ser 181	Oγ	1470	−0.407	−0.307
	120	H	H_2O(1181)	(O)		0.159	0.173
	121	H	H_2O(1181)	(O)		0.251	0.147
	151	H	Ser236	(Oγ)		0.283	0.182
	166	H	Lys185	(Nζ)		0.126	0.011
	167	H	Lys185	(Nζ)		0.084	0.011
	186	H	Ser181	(Oγ)		0.271	0.166

[a] Portion: portion in the model complex. MOPAC no.: serial number of atoms in the model complex of input data for molecular orbital calculations with MOPAC 97 that are numbered by Free Wheel. PDB label: name of atoms in the 1MMD data of the Protein Data Bank. PDB labels with parentheses signifies an atom to which H was attached. PDB no.: serial number of atoms in the 1MMD data. Charge (complex): net charge of atoms in the model complex. Charge (separated): net charge of atoms in the separated systems of MgATP-2w and the cage. These data of other atoms and Cartesian coordinates of all atoms in the 1MMD data are shown in Table 1S of Supporting Information.

To restructure the MgADP−BeF_3 to be a model of MgATP, the beryllium atom Be was replaced with a phosphorus atom P and the fluorine atoms F_3 were replaced with oxygen atoms O_3. Furthermore, hydrogen atoms missing in the X-ray structures were added to the model structure, OH was added to each C terminal of the amino acid chains, and two hydrogen atoms were added to each N terminal. The charge of MgATP was set to be −2, which is thought to be reasonable in a physiological environment,[12] and that of the remaining portion of the structure to be neutral. Only hydrogen atoms were optimized with the PM3 method[13,14] in MOPAC 97. The PM3 method can be used for calculations of structures that include Mg. The optimized structure, called "model complex", was separated into two parts, "MgATP-2w" and "cage", so that we could analyze interactions between these two parts. The "2w" of MgATP-2w indicates two water molecules. These water molecules, H_2O(1001) and H_2O(1002), coordinate tightly with the Mg ion. Therefore, these were included in the MgATP portion. The cage is composed of nine amino acid residues and the other five water molecules. Further optimization of the separated systems was not performed.

Total energies, net atomic charges, coefficients of linear combination of atomic orbital (LCAO coefficients), etc. of MgATP-2w, the cage, and the model complex were calculated using the same PM3 method. Graphic images of molecular orbitals for the molecular orbital correlation diagram, etc. were visualized using WinMOPAC.

3. Results and Discussion

3.1. Calculations of the Model Complex. To determine positions of hydrogen atoms that are lost in X-ray structures and to obtain data such as total energy of the model complex, etc., a molecular orbital calculation of the model complex with positional optimization of hydrogen atoms was performed. Cartesian coordinates of all 186 atoms of the model complex are presented in Table 1S of Supporting Information. Figure 1 shows the structure of the model complex, including the positions of the hydrogen atoms. Figure 1a shows the molecular figure in a stick and ball model that displays all 186 atoms of the model complex. None of the attached hydrogen atoms transferred elsewhere after positional optimization of the hydrogen atoms. In Figure 1b, amino acid residues of the cage are shown as labels with some side chains. As shown in Figure 1b, hydrogen bonds (H-bonds) were confirmed by analyzing the positions of hydrogen atoms and distances between base atoms. Criteria of H-bonds are distances between base atoms shorter than 2.9 Å and the location of hydrogen between base atoms. All hydrogen atoms participating in H-bonds shorter than 2.9 Å were located approximately between base atoms. H-bonds near the γ-phosphate are observed between O_{40} of H_2O(1181) and O_{37} (F1, 5907, one of the nonbridging γ-phosphoryl oxygen atoms), between N_{73} (N_ζ of Lys185) and O_{37} (F1), between O_{87} (O_γ of Ser181) and O_{110} (F2, 5908, another nonbridging γ-phosphoryl oxygen atom), and between O_{63} (O_γ of Ser236) and O_{110} (F2) (the meaning of the numbers such as O_{40}, H_2O-(1181), F1, and 5907 is presented in Table 1). Distances between

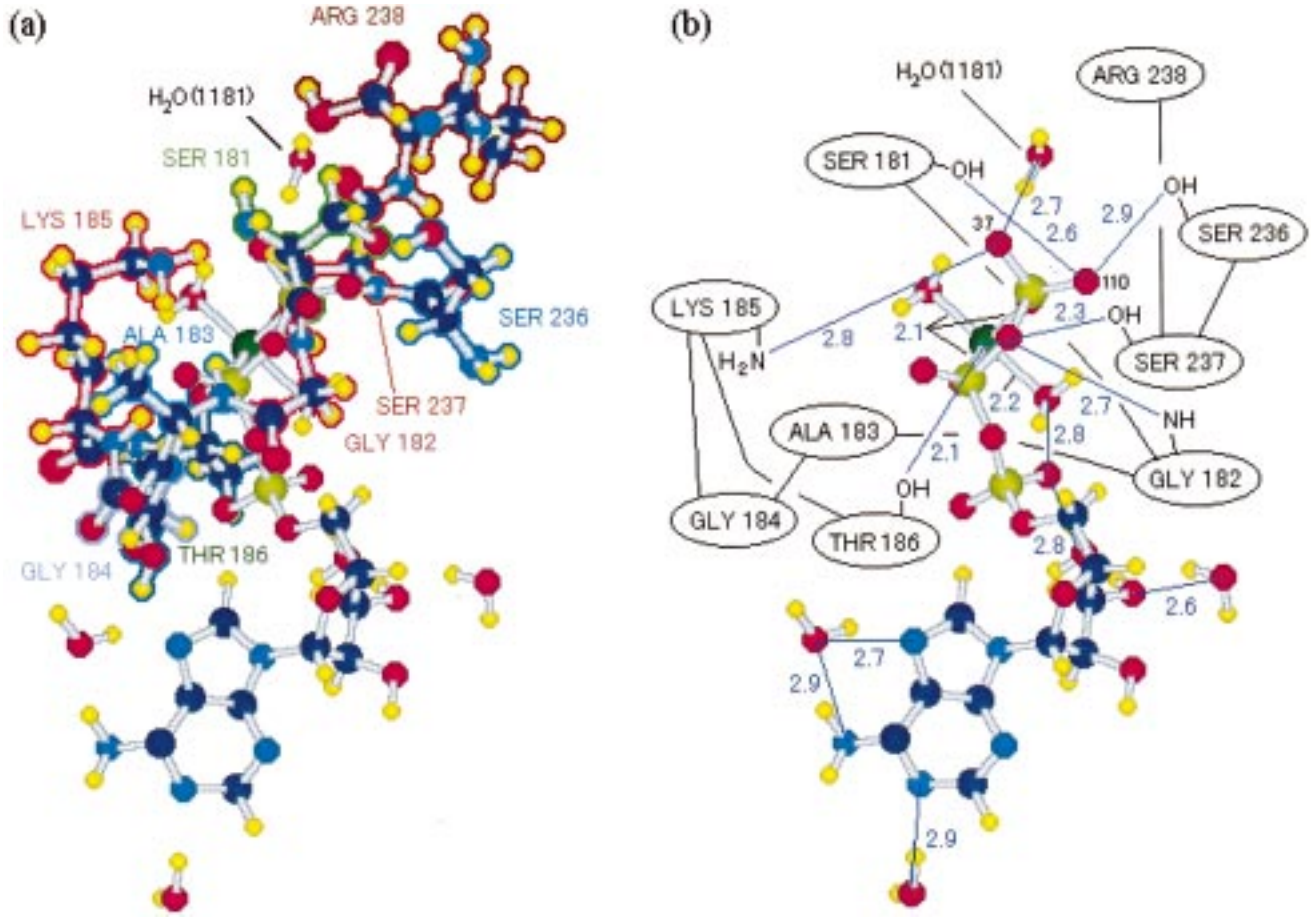

Figure 1. Molecular structure of the model complex determined by positional optimization of hydrogen atoms. The color of the balls denotes the species of the atom: dark blue, carbon; blue, nitrogen; red, oxygen; light green, phosphorus; green, magnesium; yellow, hydrogen. The gray sticks denote chemical bonds and coordinations. (a) All atoms are shown as balls, and bonds and coordinations are shown as sticks. (b) Amino acid residues of the cage are shown as labels with some side chains, and bond lengths in angstroms of H-bonds shorter than 2.9 Å and other bonds and coordinations are indicated.

H_{121} of $H_2O(1181)$ and O_{37} (F1), between H_{166} binding to N_ζ of Lys185 and O_{37} (F1), between H_{186} binding to O_γ of Ser181 and O_{110} (F2), and between H_{151} binding to O_γ of Ser236 and O_{110} (F2) are 1.8, 1.9, 1.7, and 1.9 Å, respectively.

Orbital energies of the HOMO and the lowest unoccupied molecular orbital (LUMO) of the model complex were calculated to be −4.420 and 3.062 eV, respectively. Because a negative value of the HOMO and a positive value of the LUMO are values of typical stable systems, this system is thought to be relatively stable. In this type of calculation, abnormal values, namely, positive values of HOMO or negative values of LUMO, are frequently obtained. In the present work, normal signs of values were obtained; thus, it can be assumed that the model complex satisfied the minimal condition of a stable system.

3.2. Calculations of MgATP-2w and the Cage. Molecular orbital calculations of MgATP-2w and the cage were performed. Values of total energy of MgATP-2w, the cage, and the model complex were −7042.15, −12870.78, and −19915.12 eV, respectively. Interaction energy for the complex formation was calculated to be −2.2 eV. Because the system is very large, the validity of the computer calculations was checked. For this purpose we estimated the energy of an H-bond. Dividing the value of 2.2 eV by 10 (approximate number of H-bonds involved) produces 0.22 eV/H-bond, which equals 5.0 kcal/mol. Because the H-bond energy is usually 4−5 kcal/mol, the value 2.2 eV is reasonable as the energy of the complex formation, considering other stabilization effects. This suggests that the model system is stabilized by the complex formation; in other words, the complex formation proceeds naturally in the model system.

Orbital energies of the HOMO and the LUMO of MgATP-2w are calculated to be −1.314 and 3.359 eV, respectively. Those of the cage are −8.666 and −0.093 eV, respectively. Because the orbital energy value of LUMO of the cage is slightly negative, the cage is a little electrophilic. On the other hand, the energy value of the HOMO of MgATP-2w is negative but nearly zero, so MgATP-2w can easily become an electron donor when an electrophilic object is close.

3.3. Change in Net Atomic Charge. Figure 2 shows the change in the net atomic charge of each atom in the complex formation. The change in net atomic charge, ΔQ_A, can be expressed as

$$\Delta Q_A = Q_A^{\text{complex}} - Q_A^{\text{separated}}$$

A positive ΔQ_A value indicates an incremental change in the net atomic charge.

As shown in Figure 2a, values of the net atomic charge of O_{34} (F3), one of the nonbridging γ-phosphoryl oxygen atoms to which Mg binds was greatly decreased and the values of the net atomic charge of P_{31} (P_γ) and Mg were greatly increased. As shown in Figure 2b, values of the net atomic charge of N_{73} (N_ζ of Lys185) and O_{40} of $H_2O(1181)$ greatly decreased, and those of O_{87} (O_γ of Ser181) and O_{63} (O_γ of Ser236) also

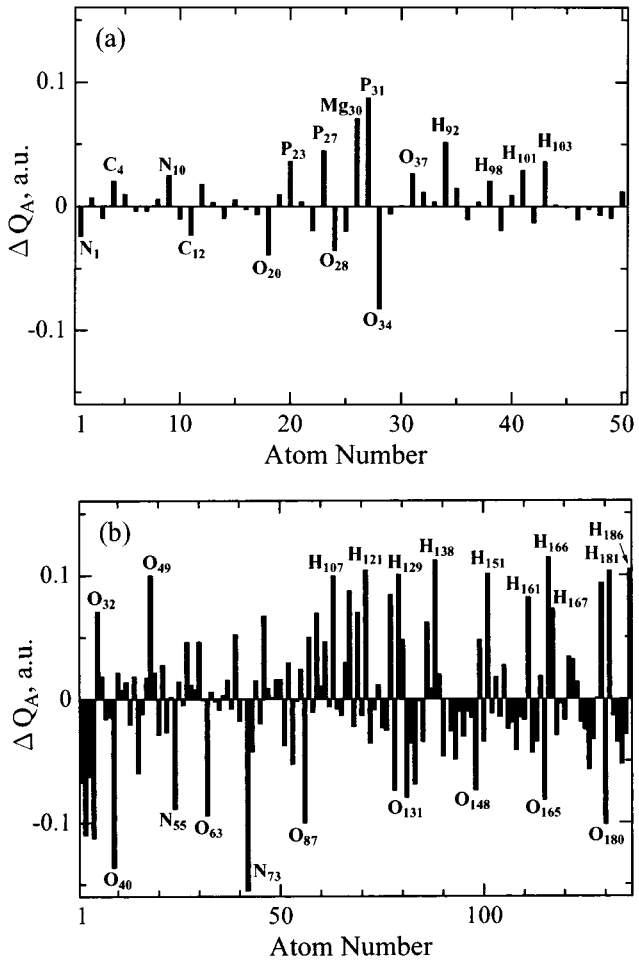

Figure 2. Change in net atomic charge of each atoms of MgATP-2w (a) and the cage (b) on the complex formation. $\Delta Q_A = Q_A^{complex} - Q_A^{separated}$, where Q_A is the net atomic charge of an atom and ΔQ_A is its increment. The label of the abscissa "atom number" means serial number of atoms in each portion. Numbers of the atoms (e.g., Mg_{30}, P_{31}, and O_{40}) are serial numbers of the atoms in the input data of the model complex for the molecular orbital calculations. Location of atoms can be seen in Table 1 and Table 1S in Supporting Information.

decreased. There are many atoms whose net atomic charge increased, e.g., H_{121} of $H_2O(1181)$, H_{166} and H_{167} binding to N_{73} (N_ζ of Lys185), H_{186} to O_{87} (O_γ of Ser181), and H_{151} to O_{63} (O_γ of Ser236). The charge of 0.202 atomic units was totally transferred from the cage to MgATP-2w when the complex formed. Thus, charge (negative charge of electron) was transferred from MgATP-2w to the cage.

3.4. Densities of States and Molecular Orbitals. Figure 3 shows the density of states (DOS) of MgATP-2w, the cage, and the model complex. The DOS indicates the number of states (energy levels) in a certain energy width. The left-hand side of Figure 3 shows DOSs of the two separated systems. It can be seen that MOs near the HOMO of MgATP-2w and MOs near the LUMO of the cage are close to each other. On the other hand, the right-hand side of Figure 3 shows the DOS of the model complex. The interaction between occupied molecular orbitals (MO) near HOMO of MgATP-2w and unoccupied MOs near LUMO of the cage induces the charge transfer from MgATP-2w to the cage and thus contributed to stabilize the model complex. Consequently, on the right-hand side of Figure 3, MOs of the model complex do not exist near the zero energy level (the HOMO−LUMO gap is actually 7.48 eV).

Figure 4 shows the molecular orbital correlation diagram. MO 287 is the HOMO of the model complex, which is thought to

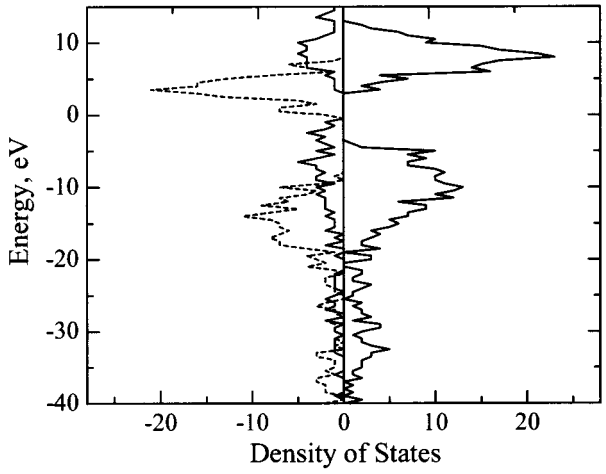

Figure 3. Densities of states of MgATP-2w, the cage, and the model complex. Left-hand side shows density of states (DOS) of two separated systems of MgATP-2w (solid lines) and the cage (broken lines). Right-hand side shows DOS of the model complex (solid lines). The DOS values in this figure are the number of states in the energy width of 0.5 eV.

be the MO most related to the chemical properties of the model complex. In Figure 4, the two MOs [MO 186 and unoccupied MO of $H_2O(1181)$] of the cage and an MO 95 (HOMO) of MgATP-2w are combined, and then three MOs [MO 285, MO 287 (HOMO), and a very high-energy unoccupied MO] of the complex are produced. In detail the following three MOs interacted.

(1) HOMO of MgATP-2w (MO 95 of MgATP-2w). This MO is occupied by two electrons and is located on energetically active parts, namely, the two nonbridging γ-phosphoryl oxygen atoms of MgATP-2w.

(2) Unoccupied MO of $H_2O(1181)$ in the Cage. $H_2O(1181)$ is neutral in the cage (calculated from the data of Table 1), so $H_2O(1181)$ does not interact with the rest of the cage without MgATP-2w. Therefore, this MO might be localized on H_2O-(1181).

(3) MO of the Cage Electronically Interactive with the Active Part of MgATP-2w (MO 186 of the Cage). This MO is occupied by two electrons and is located on N_ζ (N_{73}) and C_ϵ (C_{70}) of Lys185.

The above three MOs were reorganized to become three MOs of the model complex. Each two of the above four electrons transfer to two of the three MOs of the model complex. These two MOs are MO 285 and MO 287 of the model complex. The interaction occurs between the three MOs, namely, the MO locating on N_ζ and C_ϵ of Lys185, the MO on $H_2O(1181)$ near the γ-phosphate, and the HOMO on two nonbridging γ-phosphoryl oxygen atoms.

The mixing of states as above produces charge transfer to the unoccupied MO of $H_2O(1181)$. This MO must have the antibonding characteristic of $O_{40}-H_{121}$. The MO localized on $O_{40}-H_{121}$ is the "antibonding orbital". This charge transfer is predicted to weaken the $O_{40}-H_{121}$ bond of the water molecule. Calculated from the data of Table 1, $H_2O(1181)$ is neutral in the cage, and following the complex formation, the charge of $H_2O(1181)$ becomes -0.046. This change in charge also supports the weakening of the O−H bond. An incremental change in the positive charge of H_{121} is due to H-bonding with O_{37}, one of the nonbridging γ-phosphoryl oxygen atoms. This change in positive charge also indicates the tendency to weaken the $O_{40}-H_{121}$ bond of $H_2O(1181)$.

From the molecular orbital correlation diagram (Figure 4),

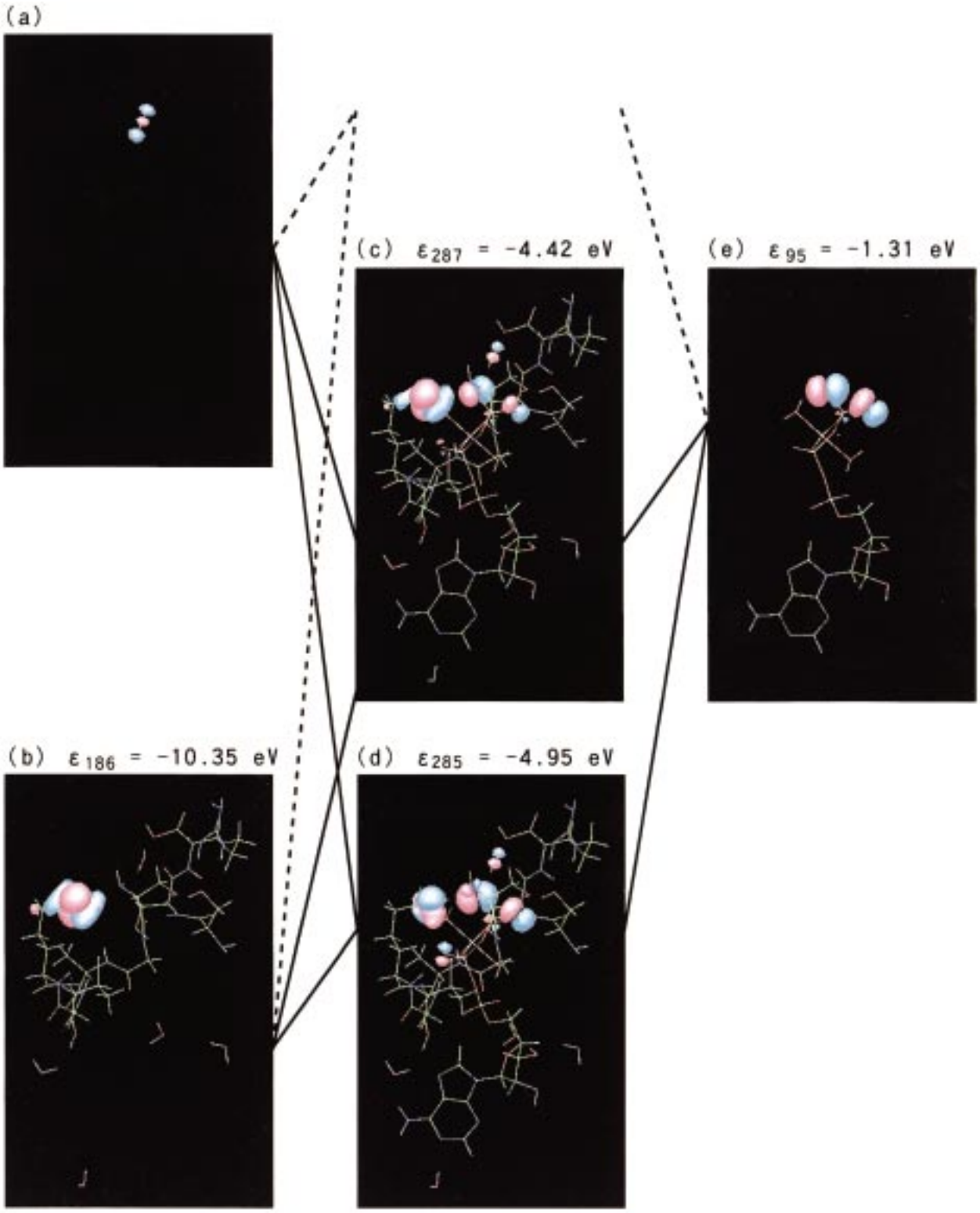

Figure 4. Molecular orbital correlation diagram. Two MOs [MO 186 (b) and the unoccupied MO of $H_2O(1181)$ (a)] of the cage in the left column and MO 95 (HOMO) of MgATP-2w (e) in the right column are combined, then three MOs [MO 285 (d), MO 287 (HOMO) (c), and a very high-energy unoccupied MO] of the complex in the central column are produced. Obtained MOs are canonical solutions of the Fock operator, so MOs are not necessarily localized. Therefore, the unoccupied MO of $H_2O(1181)$ in the cage cannot be found as a localized MO on $H_2O(1181)$. Linear combination of $2^{-1/2}(\sigma^*_{OH121} + \sigma^*_{OH120})$ and $2^{-1/2}(\sigma^*_{OH121} - \sigma^*_{OH120})$ in the cage can be thought to reproduce the antibonding orbital of $O_{40}-H_{121}$ as shown in (a). In the model complex, the H-bond between O_{40} of the water and O_{37} (γ-phosphoryl oxygen) must make the lobe on H_{121} negligibly small. The colors (red and blue) of the lobes express the opposite phase signs for MO.

$H_2O(1181)$ must be the hydrolytic water as described by Fisher et al.[8] The weakening of the O−H bond of $H_2O(1181)$ must be the start of the ATP hydrolysis. In other words, our MO calculations indicate that the interaction between MgATP-2w and the cage induces charge transfer to the antibonding orbital of $O_{40}-H_{121}$ and then promotes weakening of the O−H bond of $H_2O(1181)$, and Lys185 has an important role in the mixing of the electronic states.

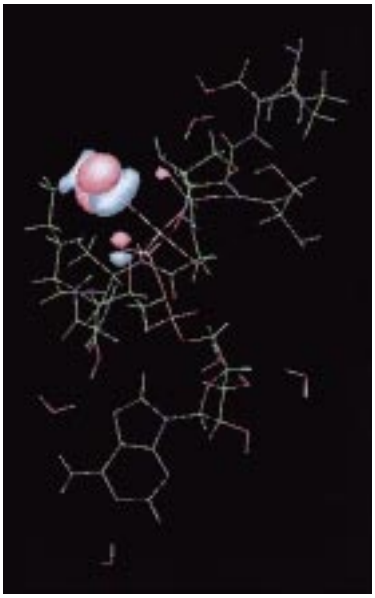

Figure 5. HOMO (MO 287) of another model complex for MgADP−BeF_3-S1Dc. The same part of MgADP−BeF_3-S1Dc in the model complex was used to compare MOs of this structure with those of the model complex. Its energy is −4.60 eV. The lobes on H_2O(1181) have disappeared, and those on nonbridging oxygen atoms of γ-phosphate have almost disappeared.

To confirm this conclusion, molecular orbitals of the same type of model complex constructed from original MgADP−BeF_x-S1Dc were calculated. The MO 287 (HOMO) of the model complex of MgADP−BeF_3-2w and the cage is shown in Figure 5. There were no lobes on H_2O(1181) and tiny lobes on the nonbridging γ-phosphoryl oxygen atoms. This fact is reasonable because MgADP−BeF_3 is stable. Thus, we can conclude that H_2O(1181) is the hydrolytic water molecule in the myosin−MgATP complex.

3.5. Hypothesis of Initial Part of the Mechanism of the ATP Hydrolysis. The MgADP−BeF_3-S1Dc structure mimics the ATP bound state.[8] In other words, the model structure can be thought to reproduce a structure of the initial phase of ATP hydrolysis. The possible initial mechanisms of the ATP hydrolysis, estimated by MO calculations, are proposed as follows:

Step 1. Formation of the complex of MgATP-2w and the cage induces charge transfer to the antibonding orbital of $O_{40}-H_{121}$ of H_2O(1181) and then promotes weakening of the $O_{40}-H_{121}$ bond. This is strongly suggested from the results of our calculations.

Step 2. We consider two schemes for this second step.

A. As shown in Figure 6, H_2O(1181) directly binds to the γ-phosphate; thus, ATP itself functions as a base, as in GTP hydrolysis by $p21^{ras}$ [15] and by transducin α.[16] As mentioned above, there is an H-bond between O_{40} of H_2O(1181) and O_{37} (one of the nonbridging γ-phosphoryl oxygen atoms); thus, H_{121}^+ might transfer to O_{37}. This proton transfer was confirmed by the fact that the positional optimization calculation of all hydrogen atoms after moving H_{121} from H_2O(1181) to one of the nonbridging γ-phosphoryl oxygen atoms did not induce transfer of the H^+ elsewhere. Therefore, it is possible that H_{121}^+ of H_2O(1181) directly transfers to γ-phosphate. After H_{121}^+ of H_2O(1181) binds to O_{37}, the remaining $O_{40}H_{120}^-$ binds to P_γ because γ-phosphate has become more accessible for OH^- after H^+ binding to the oxygen atom. In this case, an amino acid, Ser236 or Ser181, can be thought to stabilize the pentavalent phosphorus of the transition state similar to the mechanisms of GTP hydrolysis by $p21^{ras}$ [17] and by transducin α.[16]

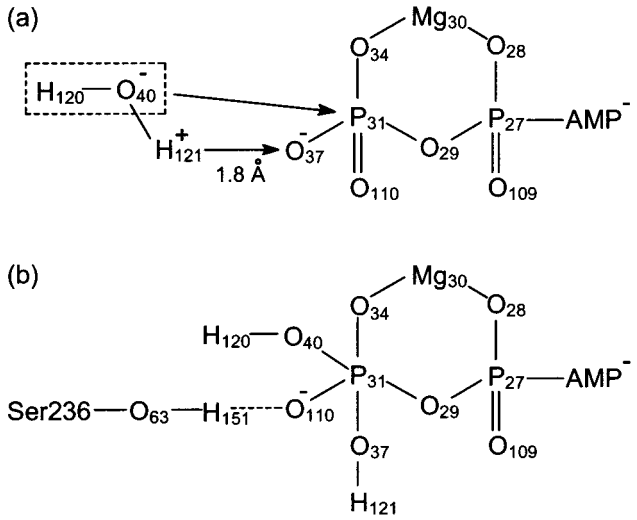

Figure 6. Schematic diagrams of a mechanism of the initial part of ATP hydrolysis mentioned in step 2A. (a) The water H_2O(1181) (H_{121}^+ and $O_{40}H_{120}^-$) binds directly to the γ-phosphate, while ATP works as a base. The proton H_{121}^+ of H_2O(1181) transfers to O_{37}, a nonbridging γ-phosphoryl oxygen atom, and then the remaining OH^- of H_2O(1181) transfers to the γ-phosphorus P_{31}. (b) An amino acid (Ser236 as an example in this figure) stabilizes the pentavalent phosphorus. Schematic diagram with Ser181 is qualitatively the same as in (b).

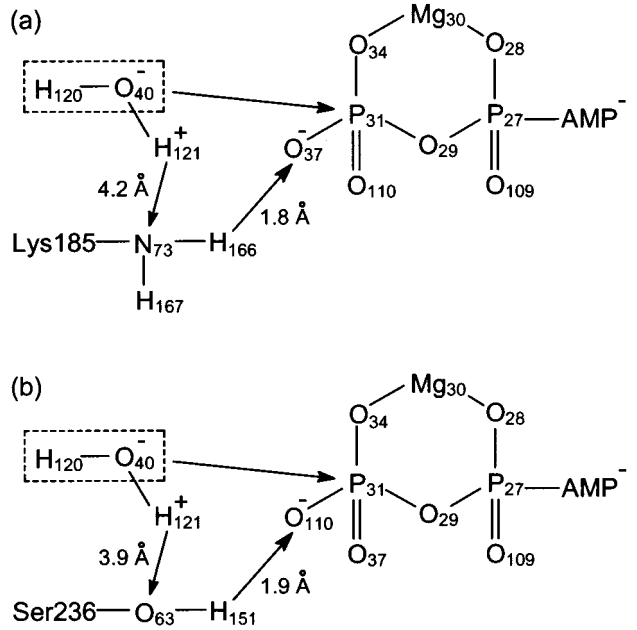

Figure 7. Schematic diagrams of another mechanism of the initial part of ATP hydrolysis mentioned in step 2B. (a) The nucleophilic atom of an amino acid residue [N_{73} (N_ζ) of Lys185] receives the H_{121}^+, and then H_{166}^+, binding already to the amino acid, is transferred to O_{37}, a nonbridging γ-phosphoryl oxygen atom. Simultaneously, the remaining $O_{40}H_{120}^-$ of H_2O(1181) is transferred to the γ-phosphorus P_{31}. (b) In the case of Ser236 instead of Lys185, the proton H_{121}^+ is transferred to O_{63} (O_γ), and then H_{151}^+ is transferred to O_{110}, another nonbridging γ-phosphoryl oxygen atom. Schematic diagram with Ser181 is qualitatively the same as in (b). In the case of Ser181, the proton H_{121}^+ is transferred to O_{87} (O_γ) beyond 4.0 Å, and then H_{186}^+ is transferred to O_{110} beyond 1.7 Å.

B. An alternative scheme can be considered. As shown in Figure 7, one of three amino acids, Lys185, Ser236, and Ser181, receives a proton H^+ from H_2O(1181), and then the H^+ already bound to the amino acid is transferred to one of the nonbridging oxygen atoms of the γ-phosphate O_{37} or O_{110}. Simultaneously, the remaining OH^- of H_2O(1181) is transferred to the γ-phos-

phorus. Thus, it can be thought that the catalytic amino acid, Lys185, Ser236, or Ser181, has two roles, one as a base and the other as an acid, and helps both H^+ and OH^- of H_2O(1181) to be transferred to the γ-phosphate. From a molecular orbital correlation diagram (Figure 4), Lys185 appears to be the amino acid that has the roles, but from the data of change in net atomic charge (Figure 2b) Ser236 and Ser181 are also candidates. The above proton transfer was confirmed by the fact that positional optimization calculations of all hydrogen atoms after moving H_{121}^+ from H_2O(1181) to each amino acid induced a proton H^+ already bound to the amino acid to move to a nonbridging γ-phosphoryl oxygen, O_{37} (F1, 5907) in the case of Lys185 or O_{110} (F2, 5908) in the case of Ser236 and Ser181. Fisher et al. described a similar scheme with Ser236 as the amino acid in Figure 8 of ref 8.

Step 3. After the H^+ and OH^- of H_2O(1181) binds to γ-phosphate, the bond of $P_\gamma-OP_\beta$ breaks, and simultaneously, the Mg ion is transferred to coordinate to both the α-phosphate and the β-phosphate. This third step is currently only a speculation. It is also possible that breaking of the $P_\gamma-OP_\beta$ bond occurs at the same time as binding of the H_2O to γ-phosphate.

For the mechanism of the proton transfer (in step 2), Fisher et al. also described a mechanism similar to case A but preferred a mechanism similar to case B.[8] We prefer the direct proton-transfer mechanism of case A only because there is an H-bond between O_{40} of H_2O(1181) and O_{37} and because O_{37} is closer to O_{40} than O_γ of Ser236.

4. Conclusion

The positions of the hydrogen atoms were determined by optimization with a semiempirical molecular orbital program MOPAC 97, and hydrogen bonds were studied mainly between MgATP-2w and the cage. From the change in total energy, the model system is stabilized by the formation of the complex of MgATP-2w and the cage. Analysis of the electronic states of the model structure revealed that the HOMOs indicate that the reaction site of the ATP hydrolysis is the nonbridging γ-phosphoryl oxygen atoms in the model and confirmed that H_2O-(1181) is the hydrolytic water. Thus, hypothetical schemes of the initial phase of the hydrolysis are proposed. In the future, molecular orbital calculations will confirm the detailed mechanisms of the hypothesis. Furthermore, the molecular orbital calculations of the transition states of the ATP hydrolysis will be performed.

Acknowledgment. The molecular orbital calculations of the MOPAC 97 PM3 method were performed using WinMOPAC, version 2 of Fujitsu Co. at Chiba, Japan (http://www.winmopac.com/). Graphic images of molecular orbitals were also visualized with this software. Input data for the software were produced and Figure 1 was depicted using the molecular modeling software Free Wheel, version 0.57Q of Butch Software Studio at Sagamihara, Japan (http://www.sf.airnet.ne.jp/~butch/indexe.html).

Supporting Information Available: Table 1S listing locations, Cartesian coordinates, and net atomic charges of all 186 atoms in the model complex. This material is available free of charge via the Internet at http://pubs.acs.org.

References and Notes

(1) Cooke, R. *Physiol. Rev.* **1997**, *77*, 671.
(2) Fukui, K.; Morokuma, K.; Nagata, C. *Bull. Chem. Soc. Jpn.* **1960**, *33*, 1214.
(3) Fukui, K.; Imamura, A.; Nagata, C. *Bull. Chem. Soc. Jpn.* **1963**, *36*, 1450.
(4) Kothekar, V.; Tyagi, R. S.; Mishra, R. K. *Indian J. Biochem. Biophys.* **1973**, *10*, 279.
(5) Kothekar, V.; Mishra, R. K. *Indian J. Biochem. Biophys.* **1974**, *11*, 259.
(6) Yoshikawa, K.; Shinohara, Y.; Terada, H.; Kato, S. *Biophys. Chem.* **1987**, *27*, 251.
(7) Tajima, M.; Honda, M. *J. Mol. Struct.: THEOCHEM* **1991**, *228*, 201.
(8) Fisher, A. J.; Smith, C. A.; Thoden, J. B.; Smith, R.; Sutoh, K.; Holden, H. M.; Rayment, I. *Biochemistry* **1995**, *34*, 8960.
(9) Fukui, K.; Yonezawa, T.; Nagata, C.; Shingu, H. *J. Chem. Phys.* **1954**, *22*, 1433.
(10) Pople, J. A.; Beveridge, D. L. *Approximate Molecular Orbital Theory*; McGraw-Hill: New York, 1970.
(11) Smith, C. A.; Rayment, I. *Biophys. J.* **1996**, *70*, 1590.
(12) Saenger, W. *Principles of Nucleic Acid Structure*; Springer-Verlag: New York, 1987; Chapter 5.
(13) Stewart, J. J. P. *J. Comput. Chem.* **1989**, *10*, 209, 221.
(14) Stewart, J. J. P. *J. Comput. Chem.* **1991**, *12*, 320.
(15) Schweins, T.; Langen, R.; Warshel, A. *Nature Struct. Biol.* **1994**, *1*, 476.
(16) Sondek, J.; Lambright, D. G.; Noel, J. P.; Hamm, H. E.; Sigler, P. B. *Nature* **1994**, *372*, 276.
(17) Schweins, T.; Geyer, M.; Scheffzek, K.; Warshel, A.; Kalbitzer, H. R.; Wittinghofer, A. *Nature Struct. Biol.* **1995**, *2*, 36.